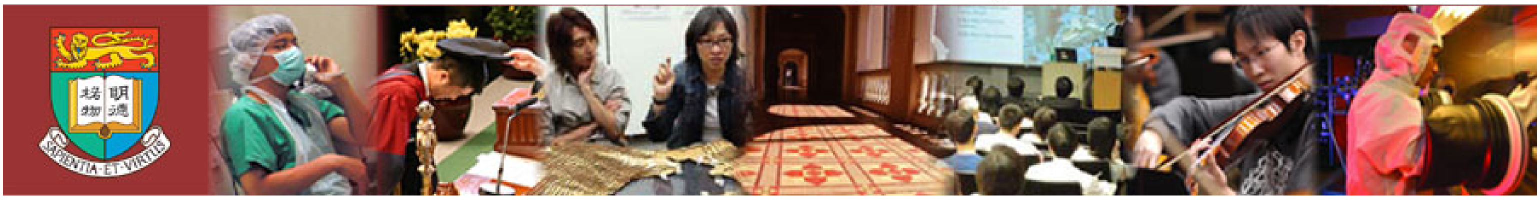

Title	**A novel wideband bandpass power divider with harmonic-suppressed ring resonator**
Author(s)	**Gao, S; Sun, S; Xiao, S**
Citation	**IEEE Microwave and Wireless Components Letters, 2013, v. 23, p. 119-121**
Issued Date	**2013**
URL	**http://hdl.handle.net/10722/189069**
Rights	**IEEE Microwave and Wireless Components Letters. Copyright © IEEE.**

A Novel Wideband Bandpass Power Divider With Harmonic-Suppressed Ring Resonator

Shan Shan Gao, *Student Member, IEEE*, Sheng Sun, *Senior Member, IEEE*, and Shaoqiu Xiao, *Member, IEEE*

***Abstract*—A simple stub-loaded ring resonator is presented as a novel wideband bandpass power divider with good in-band responses and out-of-band harmonic suppression. The first two resonances of the ring resonator are excited and employed to construct a wideband passband. By adjusting the length of loaded open stubs, four transmission zeros can be generated in the lower and upper stopbands. After installing three coupled-line sections at one input port and two output ports along the ring, additional two in-band poles and one upper-stopband transmission zero are further introduced. Subsequently, total five transmission zeros are utilized to improve the passband selectivity and suppress the high-order harmonic. In addition, a single resistor is properly placed between two output ports to ensure the isolation. Finally, a prototype power divider is fabricated and verified experimentally with attractive bandpass features.**

***Index Terms*—Bandpass power divider, harmonic suppression, open stub, ring resonator, transmission zero.**

I. Introduction

As a fundamental passive component, the power divider has been widely used in microwave and millimeter communication systems such as antenna feed networks, phase shifters, and power amplifiers. Up to date, the *Wilkinson* power divider is the most popular one, which has a simple layout and excellent isolation between two output ports [1]. However, the major drawbacks of the conventional *Wilkinson* power divider are the narrow fractional bandwidth and the presence of harmonics due to the adoption of the quarter-wavelength transmission lines. With the rapid growth of wideband communications, there has been a sustained increase in the demand of the wideband power divider design. A few types of power divider have been proposed to extend the bandwidth [2]–[4]. A wideband response can be achieved by cascading multi-section matching networks at two output ports of a single-stage power divider [2]. However, this straightforward method increases the total size of the circuit and requires more resistors for isolation. Based on tight parallel-coupled lines [3] or wideband microstrip-to-slotline transition [4], the ultra-wideband (UWB) power dividers were implemented. Unfortunately, the upper stopband bandwidth is relatively narrow. On the other hand, a low-pass power divider with wide upper stopband was realized by installing shunt stubs along branch-line sections and two extended lines between two output ports [5]. However, good isolation can be only achieved at the resonance around the cut-off frequency of low-pass response.

In this paper, a wideband bandpass power divider using a simple harmonic-suppressed ring resonator is presented. By arranging two open-circuited stubs and three coupled-line sections around the ring resonator, the first four resonances can be moved to lower frequencies and utilized together to form a wide passband along two signal paths simultaneously. Meanwhile, total five transmission zeros can be introduced at dc and upper stopband. Then, the first spurious harmonic near the wide passband can be fully suppressed, thus widening the upper stopband bandwidth. To verify our proposal, a prototype bandpass power divider is finally designed, fabricated and measured to show the good bandpass responses and wide upper stopband.

II. Bandpass Power Divider Design

Fig. 1 shows the schematic of the proposed bandpass power divider. It consists of a two-way symmetry ring resonator with four branch-line sections, two open-circuited stubs, and a single resistor (R). Z_i $(i = 1, 2, 3, 4)$ represents the characteristic impedances of each transmission line section, whereas θ_i $(i = 1, 2, 3, 4)$ indicates the corresponding electrical lengths. When a signal arrives at one input port (Port 1), its power can be divided into two parts and reaches in-phase at two output ports (Port 2 and Port 3) over the operation band. Based on the even- and odd-mode analysis, two of half circuit models can be formed with ideal open- and short-circuited ends along the horizontally symmetrical plane, as shown in Fig. 2. Then, the theoretical three-port scattering parameters can be easily obtained as [6]

$$S_{11}(f) = S_{11}^{e}(f), \tag{1a}$$

$$S_{21}(f) = S_{31}(f) = \frac{S_{12}^{e}(f)}{\sqrt{2}}, \tag{1b}$$

$$S_{23}(f) = \frac{(S_{22}^{e}(f) - S_{22}^{o}(f))}{2}, \tag{1c}$$

$$S_{22}(f) = S_{33}(f) = \frac{(S_{22}^{e}(f) + S_{22}^{o}(f))}{2} \tag{1d}$$

which can be analytically derived from the $ABCD$-matrix for even- and odd-mode circuit models. It is important to notice that the transmission coefficients in each transmission path, i.e., S_{21} and S_{31}, are only related to the even-mode scattering parameters. Thus, the transmission poles can be determined from the

Manuscript received August 31, 2012; revised November 30, 2012; accepted January 27, 2013. Date of publication February 13, 2013; date of current version March 07, 2013. This work was supported by The University of Hong Kong under Seed Funding Grant 201101159011 and 201109160010.

S. S. Gao is with the Department of Electrical and Electronic Engineering, The University of Hong Kong, Hong Kong SAR, China and also with the University of Electronic Science and Technology of China, Chengdu, China.

S. Sun is with the Department of Electrical and Electronic Engineering, The University of Hong Kong, Hong Kong SAR, China (e-mail: sunsheng@ieee.org).

S. Xiao is with the University of Electronic Science and Technology of China, Chengdu, China.

Color versions of one or more of the figures in this paper are available online at http://ieeexplore.ieee.org.

Digital Object Identifier 10.1109/LMWC.2013.2244873

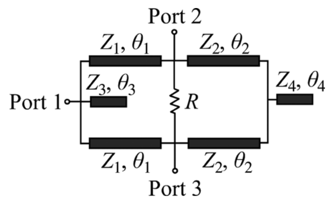

Fig. 1. Schematic of the proposed wideband bandpass power divider.

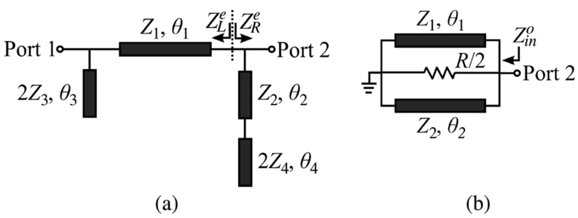

Fig. 2. (a) Even-mode circuit model. (b) Odd-mode circuit model.

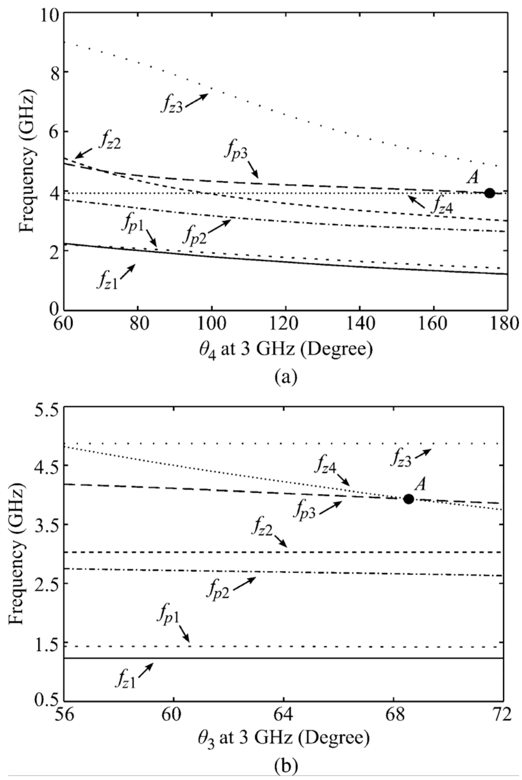

Fig. 3. Frequency locations of transmission poles and zeros versus electrical lengths of two open-circuited stubs. (a) When $\theta_3 = 68.7^\circ$ at 3 GHz. (b) When $\theta_4 = 176^\circ$ at 3 GHz. ($Z_1 = 91.4\ \Omega$, $Z_2 = Z_3 = 115.1\ \Omega$, and $Z_4 = 135.4\ \Omega$).

resonant condition of the equivalent even-mode circuit model in Fig. 2(a), which is given by

$$Z_L^e + Z_R^e = 0 \tag{2}$$

where

$$Z_L^e = \frac{Z_1(2Z_3 - Z_1 \tan\theta_1 \tan\theta_3)}{j(Z_1 \tan\theta_3 + 2Z_3 \tan\theta_1)} \tag{3}$$

and

$$Z_R^e = \frac{Z_2(2Z_4 - Z_2 \tan\theta_2 \tan\theta_4)}{j(Z_2 \tan\theta_4 + 2Z_4 \tan\theta_2)} \tag{4}$$

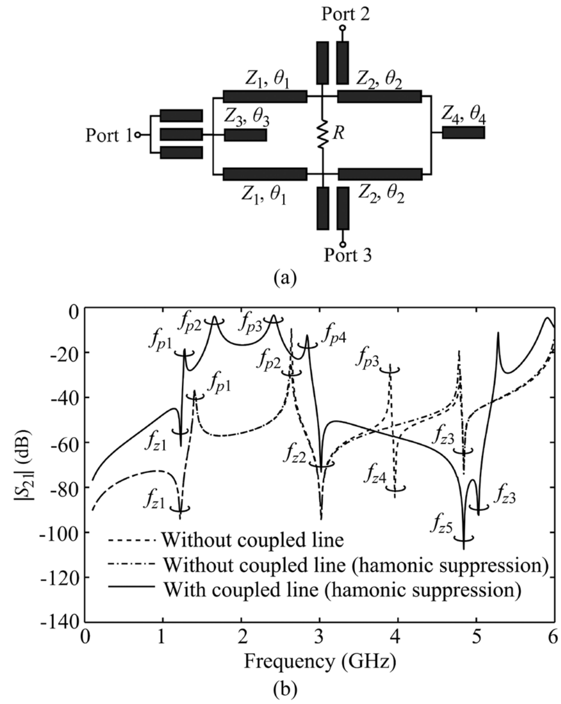

Fig. 4. Proposed power divider with coupled-line sections. (a) Schematic. (b) Frequency responses of S-magnitudes under the weak coupling.

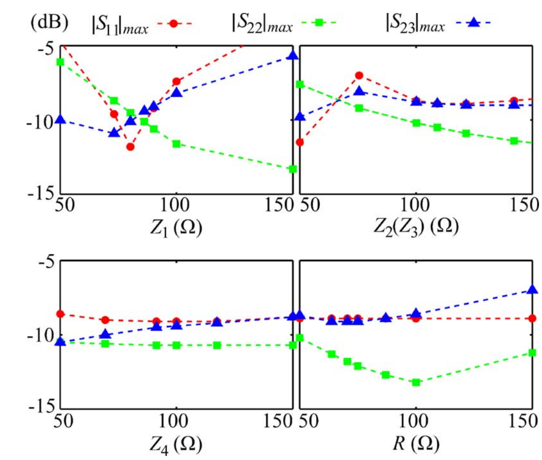

Fig. 5. Maximum reflections and isolations versus impedances (Z_i) and loaded resistor (R).

are the input impedances looking into left- and right-hand side from the reference plane.

On the other hand, the transmission zeros can be found by letting the input impedances of the two open-circuited stubs equal to zero, as follows:

$$\frac{Z_2(2Z_4 - Z_2 \tan\theta_2 \tan\theta_4)}{j(Z_2 \tan\theta_4 + 2Z_4 \tan\theta_2)} = 0 \quad (\text{for } f_{z1}, f_{z2}, \textit{ and } f_{z3}), \tag{5}$$

$$\frac{2Z_3}{j \tan\theta_3} = 0 \quad (\text{for } f_{z4}). \tag{6}$$

In this design, θ_1 and θ_2 are both chosen as 90° $(\theta_1 = \theta_2)$. Fig. 3 shows the obtained frequency distributions of the three transmission poles (f_{p1}, f_{p2}, and f_{p3}) and four transmission zeros (f_{z1}, f_{z2}, f_{z3}, and f_{z4}) versus the electrical length θ_3 and θ_4, which are equivalently measured at 3 GHz. As shown in Fig. 3(a), the first three resonances of the ring resonator at f_{p1}, f_{p2}, and f_{p3} are shifted to lower frequencies as θ_4 increases.

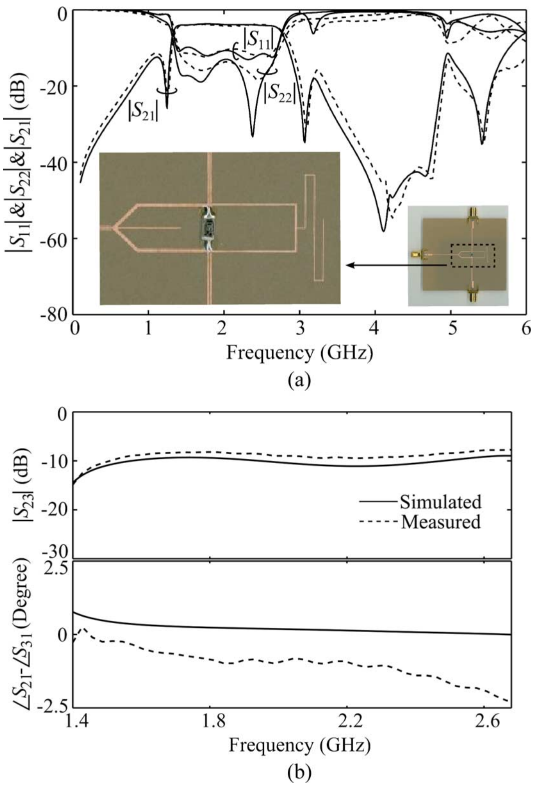

Fig. 6. Simulated and measured results. (a) S-Magnitudes. (b) Ports isolation and output phase difference with a resistor of 56 Ω in the measurement.

TABLE I
COMPARISON AMONG PUBLISHED AND PROPOSED DIVIDERS

Techniques	In-band $\lvert S_{21}\rvert_{min}$	In-band $\lvert S_{11}\rvert_{max}$	Upper Stopband Bandwidth
UWB [3]	-1.9-3 dB	-11.5 dB	24% @ -9.7 dB
Multilayer [4]	-1.9-3 dB	-10.7 dB	26.4% @ -17 dB
Proposed	-1.4-3 dB	-10.1 dB	49.4% @ -15.8 dB

Here, the first two resonances would be utilized to form a wide passband with a center operating frequency at the middle of two resonances. Here, θ_4 is set to around half-wavelength, when the two transmission zeros (f_{z1} and f_{z2}) can be well allocated at two sides of the passband. On the other hand, the three transmission zeros (f_{z1}, f_{z2}, and f_{z3}) obtained from (5) are controlled by the electrical length θ_4, while another transmission zero (f_{z4}) obtained from (6) can be almost independently controlled by the electrical length of θ_3, which could be utilized to suppress the third resonance at f_{p3}, as shown in Fig. 3(b) at point-A. Thus, θ_3 is set to 68.7° for harmonic-suppression, while the center frequency (θ_0) of the passband is allocated at 61.2°. It should be noted that θ_1 is no longer 90° at the center operating frequency, which implies a size reduction of the proposed power divider in comparison with the traditional *Wilkinson* power divider with $\theta_1 = 90°$.

In order to improve the dc and upper stopband rejections and in-band performance, three coupled-line sections are further installed at one input port and two output ports, respectively. Fig. 4 shows the corresponding schematic and S-magnitudes of the proposed power divider under the weak coupling. We can notice that the two higher resonances at f_{p3} and f_{p4} can also be shifted to lower frequencies and utilized together to form a four-pole passband after installing the coupled-line sections. Meanwhile, a higher-order harmonic around 3.9 GHz is fully suppressed by the transmission zero at f_{z4}, which is similar as the case without coupled-line sections as shown in Fig. 4(b). Moreover, two transmission zeros are introduced at dc and the upper stopband (f_{z5}) with the installation of coupled-line section.

Since θ_1 and θ_2 are no longer 90°, it is difficult to achieve the perfect impedance matching over the wide passband. Thus, further optimization is still preferred to obtain a good wideband reflection and isolation levels. Fig. 5 shows the maximum in-band reflections ($|S_{11}|_{max}$ and $|S_{22}|_{max}$) and isolation ($|S_{23}|_{max}$) versus impedances (Z_i) and loaded resistor (R), respectively. As a design example, $Z_1 = 91.4\ \Omega$, $Z_2 = Z_3 = 115.1\ \Omega$, and $Z_4 = 135.4\ \Omega$, $R = 56\ \Omega$ are finally selected in this work.

III. Experimental Results

To verify our proposal, a prototype wideband bandpass power divider is designed and implemented on a substrate with a dielectric constant of 4.8 and a substrate thickness of 0.8 mm. Fig. 6 shows the simulated and measured frequency responses and phase difference of the proposed power divider. Good agreement between them has been achieved. The measured $|S_{11}|$ is greater than 10.14 dB over the frequency range from 1.41 to 2.68 GHz, with 62% fractional bandwidth at the center frequency of 2.05 GHz. With the help of the four transmission zeros in the upper stopband, the measured upper-stropband rejection is better than 15.81 dB from 2.98 to 4.93 GHz. In addition, the measured phase difference of $\pm 2.5°$ between the output ports is observed in the entire passband. Table I compares measured in-band performance and upper stopband bandwidths for published and our proposed bandpass power divider. In addition, the loss just above transmission band-edge is primarily due to the conductor and radiation losses, which can be further improved after packaging and thicker substrate with wide conductor width is used.

IV. Conclusion

In this paper, a novel wideband bandpass power divider with harmonic-suppression has been proposed using a simple stub-loaded ring-type resonator. Multiple in-band transmission poles and out-of-band transmission zeros have been achieved to ensure good passband and wide upper stopband performance.

References

[1] E. J. Wilkinson, “An n-way hybrid power divider,” *IRE Trans. Microw. Theory Tech.*, vol. 8, no. 1, pp. 116–118, Jan. 1960.
[2] S.-W. Lee, C.-S. Kim, K. S. Choi, J.-S. Park, and D. Ahn, “A general design formula of multi-section power divider based on singly terminated filter design theory,” in *IEEE Microw. Symp. Dig.*, Jun. 2001, pp. 1297–1300.
[3] S. W. Wong and L. Zhu, “Ultra-wideband power divider with good in-band splitting and isolation performances,” *IEEE Microw. Wireless Compon. Lett.*, vol. 18, no. 8, pp. 518–520, Aug. 2008.
[4] K. Song and Q. Xue, “Novel ultra-wideband (UWB) multilayer slotline power divider with bandpass response,” *IEEE Microw. Wireless Compon. Lett.*, vol. 20, no. 1, pp. 13–15, Jan. 2010.
[5] K.-K. M. Cheng and W.-C. Ip, “A novel power divider design with enhanced spurious suppression and simple structure,” *IEEE Trans. Microw. Theory Tech.*, vol. 58, no. 12, pp. 3903–3908, Dec. 2010.
[6] H.-R. Ahn, *Asymmetric Passive Components in Microwave Integrated Circuits*. Hoboken, NJ, USA: Wiley, 2006, p. 165.